

# Ising versus XY anisotropy in frustrated $R_2Ti_2O_7$ compounds as seen by polarized neutrons

H. Cao<sup>1</sup>, A. Gukasov<sup>1</sup>, I. Mirebeau<sup>1</sup>, P. Bonville<sup>2</sup>, C. Decorse<sup>3</sup> and G. Dhalenne<sup>3</sup>.

<sup>1</sup>Laboratoire Léon Brillouin, CEA-CNRS, CE-Saclay, 91191 Gif-sur-Yvette, France.

<sup>2</sup>Service de Physique de l'Etat Condensé, CEA-CNRS, CE-Saclay, 91191 Gif-Sur-Yvette, France. and

<sup>3</sup>Laboratoire de Physico-Chimie de l'Etat Solide, ICMO, Université Paris-Sud, 91405 Orsay, France.

We studied the field induced magnetic order in  $R_2Ti_2O_7$  pyrochlore compounds with either uniaxial ( $R=Ho, Tb$ ) or planar ( $R=Er, Yb$ ) anisotropy, by polarized neutron diffraction. The determination of the local susceptibility tensor  $\{\chi_{\parallel}, \chi_{\perp}\}$  provides a universal description of the field induced structures in the paramagnetic phase (2-270 K), whatever the field value (1-7 T) and direction. Comparison of the thermal variations of  $\chi_{\parallel}$  and  $\chi_{\perp}$  with calculations using the rare earth crystal field shows that exchange and dipolar interactions must be taken into account. We determine the molecular field tensor in each case and show that it can be strongly anisotropic.

PACS numbers: 71.27.+a, 75.25.+z, 61.05.fg

The pyrochlore lattice of corner sharing tetrahedra offers the best model of geometrical magnetic frustration in three dimensions. In rare earth pyrochlore titanates  $R_2Ti_2O_7$ , frustration arises from the subtle interplay of energy terms such as single ion anisotropy, exchange and dipolar interactions. Depending on the balance between these factors, one may observe spin ice ( $R=Ho, Dy$ )<sup>1,2,3</sup> or spin liquid ( $R=Tb$ )<sup>4</sup> behaviors, or complex magnetic orders stabilized by first order transitions ( $R=Er, Yb, Gd$ )<sup>5,6</sup>. A major role in the selection of the ground state is played by the single ion anisotropy that arises from the trigonal crystal electric field (CEF) at the rare earth site. At low temperature, it may result in strong axial or planar anisotropy, depending on the wave function of the ground state and of the close CEF excited states, if any.

It is now widely accepted that  $Ho, Dy$  and  $Tb$  titanates show Ising-like behavior, the magnetic moments being constrained to align along the local  $\langle 111 \rangle$  axes. The use of the Ising model for the canonical spin ices  $Ho_2Ti_2O_7$  and  $Dy_2Ti_2O_7$  in a large temperature range is justified by their extreme axial anisotropy and very high gap between the CEF ground state and excited states<sup>7,8</sup>. In  $Tb_2Ti_2O_7$ , where this energy gap is much smaller<sup>9,10</sup>, the Ising model holds only at low temperature; above 200 K, a Heisenberg-like behavior is recovered<sup>11</sup> since many CEF levels become populated. The spin liquid ground state in  $Tb_2Ti_2O_7$  transforms into antiferromagnetic (AF) order under applied pressure and/or magnetic field<sup>12,13,14</sup>. In zero field, none of these Ising titanates evidences long range magnetic ordering (LRO) down to the lowest temperature.

The  $Er$  and  $Yb$  titanates, where the easy plane for the CEF ground state is the plane perpendicular to  $\langle 111 \rangle$ <sup>5,6,15</sup>, have been labelled XY-type pyrochlores, although they do not present extreme planar anisotropy.  $Er_2Ti_2O_7$  was suggested to realize a model XY-type antiferromagnet, for which theory predicts fluctuation-induced symmetry breaking, leading to magnetic ordering. It indeed orders antiferromagnetically at 1.2 K<sup>5,16</sup>, but can be driven into a quantum disordered state by application of a magnetic field<sup>17,18</sup>. In  $Yb_2Ti_2O_7$ , a transition detected at 0.25 K<sup>19</sup> was shown by <sup>170</sup>Yb Mössbauer spectroscopy and  $\mu$ SR<sup>6</sup> to occur towards a short range correlated state. This transition is first order and consists in a sharp and strong decrease of the spin fluctuation frequency. However, a time dependent ferromagnetic order was also reported

in  $Yb_2Ti_2O_7$ <sup>20</sup>, and the application of a moderate magnetic field was shown to drive it into a stable LRO state<sup>21</sup>.

In the pyrochlore lattice, selection between Ising, Heisenberg or XY models cannot be based, as usual, on the analysis of the macroscopic properties of a single crystalline sample in a magnetic field because of the presence of four anisotropy axes, namely the  $\langle 111 \rangle$  axes. Then only an average over the four local axes can be measured by classical methods, and no direct information can be obtained about the anisotropy of the local magnetic susceptibility of the  $R$  ion, nor of the local exchange/dipolar tensor. There is thus a clear motivation to get a direct access to these quantities and to quantify the axial/planar anisotropy in the rare earth pyrochlores.

Here we show that the site susceptibility approach<sup>22</sup> developed for polarized neutron diffraction is an accurate tool for obtaining the local susceptibility tensor  $\chi$ . We present our results in two Ising-type ( $Ho_2Ti_2O_7, Tb_2Ti_2O_7$ ) and two planar-type ( $Yb_2Ti_2O_7, Er_2Ti_2O_7$ ) compounds in a large temperature range (2 K-270 K). Knowledge of the  $\chi$ -tensor allows one to determine the moment values and orientations in the field induced paramagnetic state, whatever the field direction<sup>14</sup>. The measured thermal variations of the components of  $\chi$  are quantitatively compared with calculations using CEF parameters deduced independently from inelastic neutron scattering spectra. To obtain good agreement with the data, one needs to introduce an anisotropic molecular field tensor, which takes into account both the first neighbor exchange and the dipolar coupling.

Single crystals of  $Ho_2Ti_2O_7, Tb_2Ti_2O_7, Er_2Ti_2O_7$  and  $Yb_2Ti_2O_7$  were grown by the floating-zone technique, using a mirror furnace. The crystals were characterized by zero field neutron diffraction at 100 K and 5 K. The nuclear structure factors were used to refine positional parameters, occupancy factors, isotropic temperature factors and extinction parameters, within the space group  $Fd\bar{3}m$ .

Neutron diffraction measurements were performed at the ORPHÉE reactor of the Laboratoire Léon Brillouin. Polarized neutron flipping ratios were measured on the Super-6T2 spectrometer<sup>23</sup> using neutrons of incident wavelength  $\lambda_n=1.4$  Å and polarization  $P_0=0.98$ , and on the 5C1 spectrometer ( $\lambda_n=0.84$  Å,  $P_0=0.91$ ), provided by a supermirror bender and a Heusler polarizer, respectively. For each compound, 100-200 flipping ratios were measured, at selected tempera-

tures in the range 2 - 270 K, in a magnetic field of 1 T applied parallel to the [110] direction. The minimum number of flipping ratios used in the refinements with two parameters was 30. The programs CHILSQ<sup>24</sup> were used for the least squares refinements of the flipping ratios.

Assuming a linear response, the model assigns a susceptibility tensor  $\chi$ , of rank 3x3, to each crystallographically independent site<sup>22,25</sup>. Its components  $\chi_{ij}$  depend on the site symmetry, and the magnetic moment  $\mathbf{M}^d = \chi \mathbf{H}$  induced on a R ion at the 16d site in the unit cell is not necessarily collinear with the field, since the off-diagonal elements of  $\chi$  can be non-zero. The tensor  $\chi$  has the same symmetry as the tensor  $\mathbf{u}$  describing the thermal motion of atoms. The site susceptibility can be conveniently visualized as a *magnetization ellipsoid* constructed from the six  $\chi_{ij}$  parameters in much the same way as *thermal ellipsoids* are constructed from the  $u_{ij}$  parameters. For a given ellipsoid, the radius vector gives the magnitude and direction of the magnetic moment induced by a field of 1 T rotating in space. For the space group  $Fd\bar{3}m$ , the symmetry constraints imply that  $\chi$  has only two independent matrix elements,  $\chi_{11}$  and  $\chi_{12}$ . At the 16d site, the principal axes of the magnetization ellipsoid are oriented along the four local  $\langle 111 \rangle$  axes. Their lengths are given by:  $\chi_{\parallel} = \chi_{11} + 2\chi_{12}$  and  $\chi_{\perp} = \chi_{11} - \chi_{12}$ . These susceptibility components are determined for each temperature by refining the flipping ratios.

The thermal evolutions of  $\chi_{\parallel}$  and  $\chi_{\perp}$  are shown in Figs.1-4 for the four compounds. In the insets are represented the susceptibility ellipsoids at 5 K (lower) and 250 K (upper), whose axes have been scaled by temperature to compensate for the Curie decrease, together with the magnetic moments induced by the field applied along [110]. The four R sites of a tetrahedron are then separated into two classes: the so-called  $\alpha$ -sites (the two on the left), where the angle between the field and the ternary axis is  $35.3^\circ$ , and the  $\beta$ -sites (the two on the right), where the field is perpendicular to the ternary axis<sup>26</sup>. The data were interpreted using a single ion approach, where the trigonal symmetry CEF and Zeeman Hamiltonian is written as:

$$\mathcal{H}_{CEF} = \sum_{n,m} B_n^m O_n^m - g_J \mu_B \mathbf{J} \cdot \mathbf{H}. \quad (1)$$

In this expression, the relevant coefficients are  $B_2^0$ ,  $B_4^0$ ,  $B_4^3$ ,  $B_6^0$ ,  $B_6^3$  and  $B_6^6$ , and the  $O_n^m$  operators are expressed in terms of spherical harmonics<sup>27,28</sup>, which has the advantage that the  $B_n^m$  are roughly independent of the rare earth in an isostructural series. In equation (1),  $g_J$  is the Landé factor of the rare earth. In order to take into account exchange and dipole-dipole interactions, we introduced an anisotropic molecular field tensor  $\{\lambda_{\parallel}, \lambda_{\perp}\}$  and performed a self-consistent calculation, assuming a field component of 1 T either parallel or perpendicular to the ternary axis.

The data for  $\text{Ho}_2\text{Ti}_2\text{O}_7$  are shown in Fig.1. At low temperature, the ellipsoid elongations  $\chi_{\parallel}$  increase so markedly that they degenerate into needles, while  $\chi_{\perp}$  is very small, lying at the limit of experimental precision. The induced magnetic structure is such that the  $\alpha$ -site moments point towards the field direction, while remaining along the local ternary axis, and the  $\beta$ -site moments are zero. At high temperature, on the

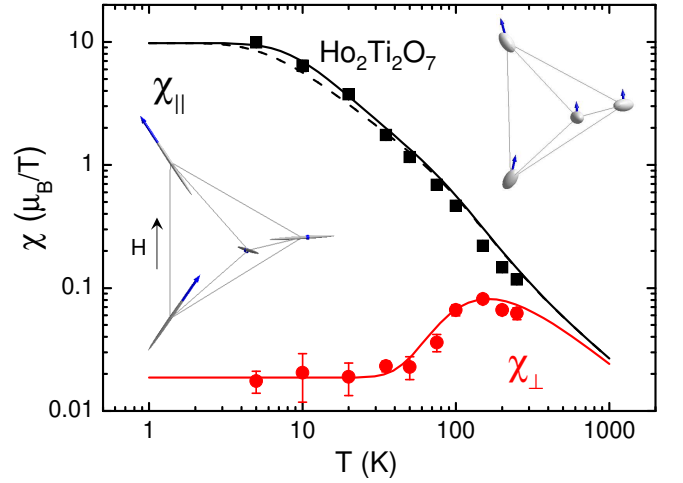


FIG. 1: (color on line).  $\text{Ho}_2\text{Ti}_2\text{O}_7$ : Susceptibility components  $\chi_{\parallel}$  and  $\chi_{\perp}$  versus  $T$ . The following CEF parameters (in K) were used<sup>7</sup>:  $B_2^0 = 791$ ,  $B_4^0 = 3188$ ,  $B_4^3 = 971$ ,  $B_6^0 = 1007$ ,  $B_6^3 = -725$  and  $B_6^6 = 1178$ . Dashed lines: CEF only calculation; solid lines: calculation including effective exchange:  $\lambda_{\parallel} = 0.05 \text{ T}/\mu_B$ ,  $\lambda_{\perp} = 0$ . For  $\chi_{\perp}$ , both lines superimpose.

contrary, the anisotropy is weaker and all the moments reorient close to the field direction. These features, and in particular the peculiar shape of  $\chi_{\perp}(T)$ , are explained by the CEF level scheme of  $\text{Ho}^{3+}$  ( $J=8$ ,  $g_J=5/4$ ) in  $\text{Ho}_2\text{Ti}_2\text{O}_7$ : the ground state is very close to the extremely anisotropic non-Kramers doublet  $|J=8; J_z=\pm 8\rangle$ , which has a moment of  $10\mu_B$  along the ternary axis and  $\chi_{\perp} = 0$ , and the first excited state lies at about 250 K above the ground state<sup>7,8</sup>. The lines in Fig.1 were calculated using the CEF parameters given in Ref.7. We find that the CEF only curves (dashed lines) yield a good agreement with the data. Due to the smallness of  $\chi_{\perp}(T)$ , no reliable value for the molecular field constant  $\lambda_{\perp}$  can be obtained. For  $\chi_{\parallel}$ , introduction of a small positive (ferromagnetic) value  $\lambda_{\parallel} = 0.05(1) \text{ T}/\mu_B$  improves the agreement with the data (see Fig.1). Since the saturated Ho magnetic moment along  $\langle 111 \rangle$  is  $\mu = 10\mu_B$ , this yields an effective field  $H_{\parallel} = \lambda_{\parallel}\mu = 0.5 \text{ T}$ . The exchange and dipolar interactions in the ground spin-ice state of  $\text{Ho}_2\text{Ti}_2\text{O}_7$  are well known at low temperature<sup>29</sup>, amounting to a positive effective exchange constant  $J_{eff} \approx 1.8 \text{ K}$ , where the dipolar contribution dominates. This is equivalent to a field  $H_{eff} \approx 0.27 \text{ T}$  along the ternary axis. An exact comparison with our result is however difficult because the magnetic structure induced by the field in  $\text{Ho}_2\text{Ti}_2\text{O}_7$  is quite different from the zero-field moment arrangement in a spin-ice, hence modifying the dipolar field at a Ho site.

The CEF anisotropy of  $\text{Tb}^{3+}$  ( $J=6$ ,  $g_J=3/2$ ) in  $\text{Tb}_2\text{Ti}_2\text{O}_7$  is considerably smaller than that of  $\text{Ho}^{3+}$  in  $\text{Ho}_2\text{Ti}_2\text{O}_7$  (see Fig.2). At room temperature,  $\text{Tb}_2\text{Ti}_2\text{O}_7$  is practically isotropic<sup>11,14,30</sup> due to the relatively large number of populated CEF levels<sup>9,10</sup>. Decreasing the temperature, it evolves progressively into an Ising type with a ratio of ellipsoid axes of the order of 10. A CEF only calculation using the parameters from Ref.10 accounts practically for the  $\chi_{\parallel}$  data, and lies somewhat above the  $\chi_{\perp}$  data. Introducing an anisotropic  $\lambda$ -

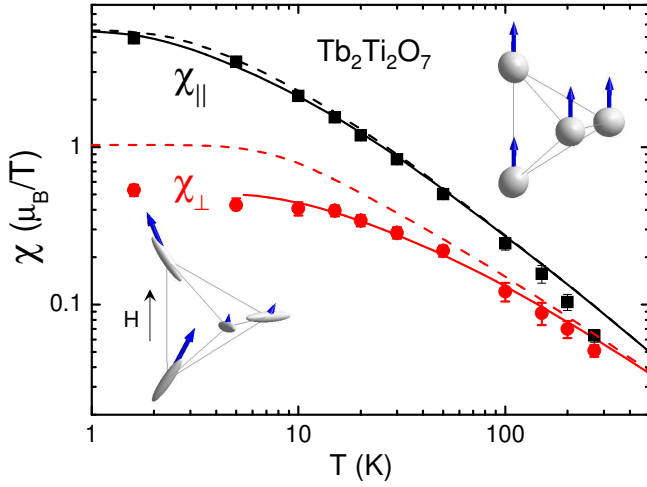


FIG. 2: (color on line).  $\text{Tb}_2\text{Ti}_2\text{O}_7$ : Susceptibility components  $\chi_{||}$  and  $\chi_{\perp}$  versus  $T$ . The following CEF parameters (in K) were used<sup>10</sup>:  $B_2^0 = 712$ ,  $B_4^0 = 3400$ ,  $B_4^3 = 1200$ ,  $B_6^0 = 1130$ ,  $B_6^3 = -700$  and  $B_6^6 = 1140$ . Dashed lines: CEF only calculation; solid lines: calculation including effective exchange:  $\lambda_{||} = -0.05 \text{ T}/\mu_B$ ,  $\lambda_{\perp} = -1 \text{ T}/\mu_B$ .

tensor improves the agreement, especially for  $\chi_{\perp}$ , with the AF values:  $\lambda_{||} = -0.05(2) \text{ T}/\mu_B$  and  $\lambda_{\perp} = -1.0(2) \text{ T}/\mu_B$ . We have checked that this  $\lambda$ -tensor is coherent with the isotropic effective value  $\lambda = -0.33 \text{ T}/\mu_B$  derived in Ref.10 from the analysis of the high temperature powder susceptibility. For  $\chi_{\perp}(T)$ , the self-consistent calculation does not converge below about 5 K, which is the “ordering” temperature of the model; this is why there are no calculated points for  $\chi_{\perp}$  below 5 K in Fig.2. Both components of the  $\lambda$ -tensor, which corresponds to an effective (exchange + dipole) low temperature interaction, are found to be of AF type, in line with the position of  $\text{Tb}_2\text{Ti}_2\text{O}_7$  in the phase diagram of Ref.31. Our own previous estimation<sup>10</sup> tentatively located  $\text{Tb}_2\text{Ti}_2\text{O}_7$  in the spin ice side of this phase diagram, but it was based on the high temperature isotropic determination of  $\lambda$  and could not take into account the anisotropy of the  $\lambda$ -tensor found in the present work.

As seen from Fig.3, the anisotropy of  $\text{Er}^{3+}$  ( $J=15/2$ ,  $g_J=6/5$ ) in  $\text{Er}_2\text{Ti}_2\text{O}_7$  is rather weak, and a spherical shape for the magnetic ellipsoids is recovered above 100 K. At low temperature,  $\chi_{\perp} > \chi_{||}$ , in agreement with the planar magnetic ordering below 1.2 K found in Ref.5. The CEF parameters for  $\text{Er}_2\text{Ti}_2\text{O}_7$ , extrapolated from those in  $\text{Ho}_2\text{Ti}_2\text{O}_7$ , were refined so as to reproduce the energies of the two lowest CEF excited doublets<sup>5</sup>, at 6.3 and 7.3 meV, as well as the transverse component of the  $g$ -tensor of the ground Kramers doublet, which must match the in-plane saturated moment. The CEF parameters listed in the caption of Fig.3 meet these requirements, with  $g_{||}=2.6$  and  $g_{\perp}=6.8$  for the ground doublet, the latter value yielding  $m_{sat} = \frac{1}{2}g_{\perp}\mu_B = 3.4\mu_B$ , close to the measured value  $3\mu_B$ . The CEF only calculation of the susceptibilities shows a good first order agreement for  $\chi_{||}(T)$ , and introduction of the effective exchange improves greatly the agreement for  $\chi_{\perp}(T)$ . We find the  $\lambda$ -tensor in  $\text{Er}_2\text{Ti}_2\text{O}_7$  is also anisotropic and of AF type:  $\lambda_{\perp} = -0.45(5) \text{ T}/\mu_B$  and  $\lambda_{||} = -0.15(1) \text{ T}/\mu_B$ . The in-plane effective exchange is thus stronger than its com-

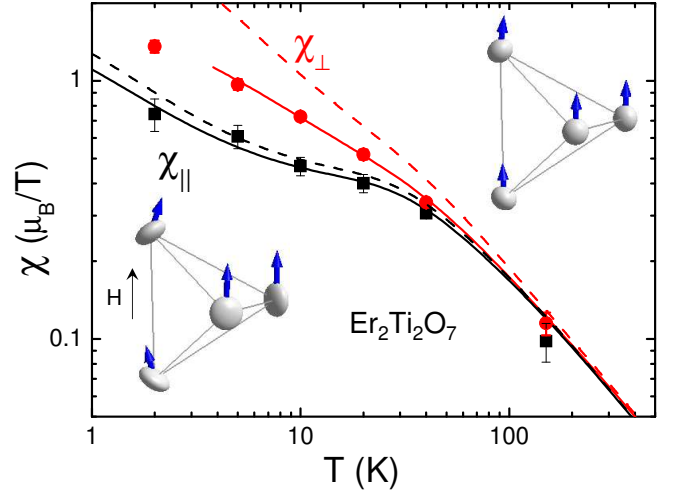


FIG. 3: (color on line).  $\text{Er}_2\text{Ti}_2\text{O}_7$ : Susceptibility components  $\chi_{||}$  and  $\chi_{\perp}$  versus  $T$ . The following CEF parameters (in K) were used (see text):  $B_2^0 = 616$ ,  $B_4^0 = 2850$ ,  $B_4^3 = 795$ ,  $B_6^0 = 858$ ,  $B_6^3 = -493$  and  $B_6^6 = 980$ . Dashed lines: CEF only calculation; solid lines: calculation including effective exchange:  $\lambda_{||} = -0.15 \text{ T}/\mu_B$  and  $\lambda_{\perp} = -0.45 \text{ T}/\mu_B$ .

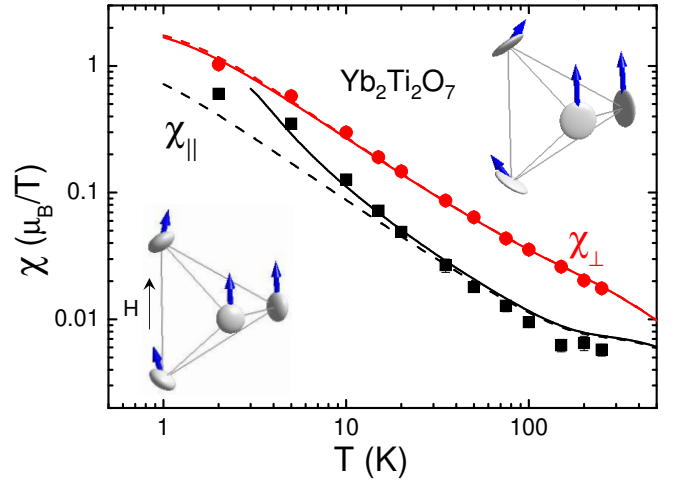


FIG. 4: (color on line).  $\text{Yb}_2\text{Ti}_2\text{O}_7$ : Susceptibility components  $\chi_{||}$  and  $\chi_{\perp}$  versus  $T$ . The following CEF parameters (in K) were used (see text):  $B_2^0 = 750$ ,  $B_4^0 = 2350$ ,  $B_4^3 = 1200$ ,  $B_6^0 = 700$ ,  $B_6^3 = -1000$  and  $B_6^6 = 700$ . Dashed lines: CEF only calculations, solid lines: calculation including effective exchange:  $\lambda_{||} = 2.5 \text{ T}/\mu_B$ ,  $\lambda_{\perp} = -0.05 \text{ T}/\mu_B$ .

ponent along the ternary axis, which reinforces the XY character determined by the CEF anisotropy.

Fig.4 shows the temperature dependence of  $\chi_{||}$  and  $\chi_{\perp}$  for  $\text{Yb}^{3+}$  ( $J=7/2$ ,  $g_J=8/7$ ) in the planar anisotropy pyrochlore  $\text{Yb}_2\text{Ti}_2\text{O}_7$ . Its magnetic ellipsoids are disk-shaped, like in  $\text{Er}_2\text{Ti}_2\text{O}_7$ , but a strong anisotropy persists up to much higher temperature because the excited Kramers doublets lie much higher in energy (700-1000 K)<sup>15</sup>. In order to calculate  $\chi_{||}(T)$  and  $\chi_{\perp}(T)$ , we used CEF parameters extrapolated from those in  $\text{Ho}_2\text{Ti}_2\text{O}_7$ . The chosen set of parameters must also reproduce the thermal variation of the  $4f$  quadrupolar moment

$Q_{4f}(T) \propto \langle 3J_z^2 - J(J+1) \rangle_T$  measured by the  $\gamma - \gamma$  Perturbed Angular Correlations technique<sup>15</sup>. The  $B_n^m$  coefficients listed in the caption of Fig.4 meet these requirements and yield a rather good agreement with the experimental data for  $\chi_{\perp}(T)$ , implying  $\lambda_{\perp} \simeq 0$ . For  $\chi_{\parallel}(T)$ , a ferromagnetic value  $\lambda_{\parallel}=2.5(5)\text{T}/\mu_B$  is needed to reproduce the data. We checked that the powder susceptibility calculated using this  $\lambda$ -tensor agrees with experiment, i.e. that it leads to an almost vanishing paramagnetic Curie temperature below 20 K<sup>15</sup>. The present set of parameters, which differs from the previous set<sup>6</sup> roughly by interchanging the  $B_4^0$  and  $B_6^0$  values, is coherent with those in the  $\text{R}_2\text{Ti}_2\text{O}_7$  family. It yields a somewhat larger  $g_{\parallel}$  value for the ground doublet (2.25 vs 1.80), which implies that the Yb moment of  $1.15\mu_B$  in the “slow fluctuation” phase below 0.25 K<sup>6</sup> probably lies along the  $\langle 111 \rangle$  axis.

R	Ho	Tb	Er	Yb
$\lambda_{\parallel}$	0.05(5)	-0.05(2)	-0.15(1)	2.5(5)
$\lambda_{\perp}$	--	-1.0(2)	-0.45(5)	0.00(5)

TABLE I: Values of the two components of the molecular field tensor (in  $\text{T}/\mu_B$ ) in the  $\text{R}_2\text{Ti}_2\text{O}_7$  compounds.

In conclusion, polarized neutron diffraction allowed us to determine the local susceptibility tensor in the  $\text{R}_2\text{Ti}_2\text{O}_7$  series,

inaccessible by macroscopic measurements in single crystals. Its temperature dependence in the paramagnetic phase cannot be entirely accounted for by the sole crystal field anisotropy: a molecular field tensor  $\lambda$  must be introduced, which encompasses exchange and dipolar interactions, and which is found to be strongly anisotropic in most compounds. The values of the  $\lambda$  components are gathered in Table I. Their sign and magnitude agree with the onset of planar AF ordering (Er) and spin ice short range order (Ho). For Yb, we find an extremely anisotropic ferromagnetic  $\lambda$ -tensor along  $\langle 111 \rangle$  with a moderate planar CEF anisotropy. By contrast, for Tb, which has a strong CEF anisotropy along  $\langle 111 \rangle$ , the  $\lambda$ -tensor is of AF type and characterized by a sizeable planar anisotropy. The anisotropy of the  $\lambda$ -tensor is likely to be due mainly to the dipole-dipole coupling in the large moment systems (Ho and Tb), but our results suggest that exchange itself is anisotropic in the small moment systems (Er and Yb), where dipolar interactions play a minor role. This could be an important ingredient for theory in  $\text{Tb}_2\text{Ti}_2\text{O}_7$  and  $\text{Yb}_2\text{Ti}_2\text{O}_7$ , where the ground state is not yet fully understood.

We thank Patrick Berthet for his support in the crystal synthesis, A. Cousson and B. Gillon for their help in the experiments. We also thank P. J. Brown for her advices in using CCSL and interesting discussions. H. Cao acknowledges financial support from the Triangle de la Physique.

- 
- <sup>1</sup> M. J. Harris, S. T. Bramwell, P. C. W. Holdsworth, and J. D. M. Champion, *Phys. Rev. Lett.* **81**, 4496 (1998).  
<sup>2</sup> A. P. Ramirez *et al.* *Nature* **399**, 333 (1999).  
<sup>3</sup> S. T. Bramwell and M. J. P. Gingras, *Science* **294**, 1495 (2001).  
<sup>4</sup> J. S. Gardner *et al.*, *Phys. Rev. Lett.* **82**, 1012 (1999).  
<sup>5</sup> J. D. M. Champion *et al.* *Phys. Rev. B* **68**, 020401(R) (2003).  
<sup>6</sup> J. A. Hodges *et al.*, *Phys. Rev. Lett.* **88**, 077204 (2002).  
<sup>7</sup> S. Rosenkranz, A. P. Ramirez, A. Hayashi, R. J. Cava, R. Siddharthan and B. S. Shastry *J. Appl. Phys.* **87** 5914 (2000).  
<sup>8</sup> Y. M. Jana and D. Ghosh *Phys. Rev. B* **61** 9657, (2000).  
<sup>9</sup> M. J. P. Gingras *et al.* *Phys. Rev. B* **62**, 6496 (2000).  
<sup>10</sup> I. Mirebeau, P. Bonville and M. Hennion *Phys. Rev. B* **76**, 184436 (2007).  
<sup>11</sup> Y. J. Kao, M. Enjalran, A. Del Maestro, H. R. Molavian, M. J. P. Gingras *Phys. Rev. B* **68**, 172407 (2003).  
<sup>12</sup> I. Mirebeau, I. N. Goncharenko, G. Dhalenne and A. Revcolevschi *Phys. Rev. Lett.* **93**, 187204 (2004).  
<sup>13</sup> K. C. Rule *et al.* *Phys. Rev. Lett.* **96**, 177201 (2006).  
<sup>14</sup> H. Cao, A. Gukasov, I. Mirebeau, P. Bonville and G. Dhalenne *Phys. Rev. Lett.* **101**, 196402 (2008).  
<sup>15</sup> J. A. Hodges, P. Bonville, A. Forget, M. Rams, K. Królas and G. Dhalenne *J. Phys.: Condens. Matter* **13** 9301, (2001).  
<sup>16</sup> A. Poole, A. S. Wills and E. Lelièvre-Berna, *J. Phys.: Condens. Matter* **19**, 452201 (2007).  
<sup>17</sup> J. P. C. Ruff *et al.* *Phys. Rev. Lett.* **101**, 147205 (2008).  
<sup>18</sup> P. A. McClarty, S. H. Curnoe and M. J. P. Gingras arXiv:0810.2483, cond-mat.str-el. (2008)  
<sup>19</sup> H. W. J. Blöte, R. F. Wielinga, W. J. Huiskamp *Physica* **43**, 549 (1969).  
<sup>20</sup> Y. Yasui *et al.*, *J. Phys. Soc. Jpn.* **72**, 3014 (2003).  
<sup>21</sup> K. A. Ross *et al.*, arXiv:0902.0329, cond-mat.str-el. (2009)  
<sup>22</sup> A. Gukasov and P. J. Brown, *J. Phys.: Condens. Matter* **14**, 8831, (2002).  
<sup>23</sup> A. Gukasov *et al.* *Physica B* **397**, 131134 (2007).  
<sup>24</sup> P. J. Brown and J. C. Matthewman, CCSL-RAL-93-009 (1993), and <http://www.ill.fr/dif/ccsl/html/ccsl/doc.html>  
<sup>25</sup> A. Gukasov, P. Rogl, P. J. Brown, M. Mihalik and A. Menovsky *J. Phys.: Condens. Matter* **14**, 8841 (2002).  
<sup>26</sup> Z. Hiroi, K. Matsuhira and M. Ogata, *J. Phys. Soc. Jpn.* **72**, 3045 (2003).  
<sup>27</sup> M. T. Hutchings, *Solid State Phys.* **16**, 227 (1964).  
<sup>28</sup> B. G. Wybourne, *Spectroscopic Properties of Rare Earths* (Interscience, New York, 1965).  
<sup>29</sup> S. T. Bramwell *et al.*, *Phys. Rev. Lett.* **87**, 047205 (2001).  
<sup>30</sup> A. Gukasov, H. Cao, I. Mirebeau and P. Bonville *Physica B*, Proceedings of PNCMI2008 (2009), in press.  
<sup>31</sup> B. C. den Hertog and M. J. P. Gingras, *Phys. Rev. Lett.* **84**, 3430 (2000)